Electronic Supplementary Material (ESI) for New Journal of Chemistry.

Supporting Information for

Copper-based Hydrogels with Dicarboxylate spacer ligands for Selective Carbon Dioxide Separation Application

Mona Al-Dossary,[*a] Harihara Padhy,[a,b] Feng Xu,[a] Ali R. Behzad,[c] Omar el Tall,[c] Alexander Rothenberger[a]

[a]*Physical Sciences and Engineering Division, King Abdullah University of Science and Technology (KAUST), Thuwal 23955-6900, Kingdom of Saudi Arabia.*

[b]*Department of Chemistry, VIT Bhopal University, Bhopal 466114, India.*

[c] *King Abdullah University of Science and Technology (KAUST), Core Labs, Thuwal, 23955-6900, Saudi Arabia*

Correspondence to: Mona Al Dossary (E-mail: mona.dossary@kaust.edu.sa)

Table of Content

Detailed experimental methods

Chemicals

Disodium adipate (TCI, ≥98%), terephthalic acid (Aldrich, ≥98%), nitrilotriacetic acid trisodium salt (Sigma Aldrich, ≥ 98%) and trisodium citrate salt (Sigma Aldrich, ≥ 98%), respectively. Sodium hydroxide ((Sigma Aldrich, ≥ 98 %), copper nitrate $Cu(NO_3)_2.3H_2O$ (Sigma Aldrich, ≥ 98 %), iron (III) nitrate ($Fe(NO_3)_3.9H_2O$) (Sigma Aldrich, ≥ 99,99 %), aluminum nitrate ($Al(NO_3)_3.9H_2O$) (Analytical reagent ≥ 99.1%) , zinc nitrate ($Zn(NO_3)_2.6H_2O$) (Sigma Aldrich, ≥ 98 %), nickel nitrate ($Ni(NO_3)_2.6H_2O$) (Sigma Aldrich, ≥ 98.5 %), cobalt nitrate ($Co(NO_3)_2.6H_2O$) (Sigma Aldrich, ≥ 98 %).

Instrumentation

FT-IR spectra. FT-IR spectra were recorded on a Thermo Nicolet iS10 FT-IR Spectrometer. Photographs were taken with a Sony Cyber-Shot DSC-W80 digital camera.

Supercritical Drying. Synthesized hydrogels were placed for solvent exchange in ethanol for 5 days, and then dried with an Autosamdri-815B instrument. During supercritical drying, samples were soaked with liquid CO_2 and flushed 6-7 times over a period of 4 h at 10 °C to completely remove the ethanol from the wet gels. Finally, dry hydrogels were obtained after supercritical drying at 35 °C.

Scanning Electron Microscopy (SEM). For the SEM images, approximately, 1 cc of hydrogel were placed for the solvent exchange with ethanol and then dried super critically with CO_2. The obtained powder samples were placed on carbon tape and taken into the instrument chamber for image capture.

Cryo-SEM. Small amount of samples (approximately 3 mm^3) were mounted vertically inside an opening onto an aluminum stub. Samples were frozen in the liquid nitrogen slush and transferred under vacuum into a PP2000T cryo preparation chamber precooled at -180 °C. To remove residual ice contamination, sample temperature was raised to -90 °C for 2 min. Frozen hydrogels were then sputter coated with 5 nm-thick platinum in an argon atmosphere at -150 °C. To fracture the frozen hydrogel, the top part of the vertically mounted sample was hit with a knife precooled at -150 °C. In order reveal the detailed structure of fractured plane, the samples were sublimed inside the

SEM chamber at -90 °C. After sublimation, samples were transferred back to the preparation chamber and sputter coated with 2.5 nm-thick platinum in an argon atmosphere at -150 °C. The samples were then transferred back to SEM cryo stage, held at -130 °C, and high quality SEM images were captured. Stereopair images were captured at 0 and -5 degree tilt and two images were merged using the FEI user interface software. In all cases, the imaging was performed using an accelerating voltage of 5 kv and working distance of 10 mm.

Rheology Experiment. The gel sample was placed on the lower plate, and frequency sweep experiments were carried out at a constant frequency of 1 rad/s at 25 °C to obtain storage or elastic modulus, *G*', and loss or viscous modulus, *G*".

The amplitude sweep measurements were carried out at a constant stress in the linear viscoelastic range. For each gel, the experiments were carried out 3 times and average values were plotted. The elastic modulus values were taken in the linear viscoelastic region, which are independent of the applied strain.

Gas Adsorption Measurements. Nitrogen adsorption and desorption isotherms were performed at 77 K. About 100–200 mg of sample was taken for each analysis. Before the analysis, samples were degassed at 343 K under vacuum ($<10^{-4}$ mbar) for 10 h. Low pressure incremental dosing of 0.1338 $mmol.g^{-1}$ (STP) and 30 s equilibration were applied as analysis conditions. BET transform plots were obtained in the 0.05 to 0.35 relative pressure (P/P_0) regions, and a correlation coefficient of 0.99999 was obtained in all of the cases while the distribution of the pore sizes was calculated using the Barrett–Joyner–Halenda (BJH) model.

Dynamic mechanical analysis.

DMA measurements were performed in the compression mode for powdered samples a dynamic mechanical analyzer (G2RSA-TA instrument) equipped with parallel plate compression clamp. The PVM/Na-MA:Cu^{2+} sample with 10:4:2.5 ratio was first critically point dried using supercritical CO_2 then it was ground to fine powder and 0.2 g were pressed in a steel die of 13 mm diameter by a pressing apparatus under ambient air for 5 min resulting in 1.1 mm thick pellet. Temperature scan was carried out from 25 °C to 250 °C with a heating rate of 5 $°C.min^{-1}$ at an angular frequency of 10 $rad.s^{-1}$.

Effects of various types of metal ions on hydrogel formation

We studied the effects of the type of metal ions used in the crosslinking of hydrogel formation by considering three factors. The first factor was the nature of the metal ion. We analyzed several metal ion salts, including copper nitrate ($Cu(NO_3)_2$) , iron nitrate ($Fe(NO_3)_3$, aluminum nitrate ($Al(NO_3)_3$), zinc nitrate ($Zn(NO_3)_2$, nickel nitrate ($Ni(NO_3)_2$), and cobalt nitrate ($Co(NO_3)_2$). The second factor was the polymer-to-metal molar ratio, which we varied for each metal to determine the optimal polymer-to-metal-ion ratio needed for hydrogel formation. The third factor was the effect of the pH of the solution on the crosslinking and hydrogel structure. We studied this effect by varying the pH of the starting polymer solution. The pH and amount of NaOH were previously found to affect the crosslinking density.[1] We also studied the solubility of the metal ions in the solution, the formation of hydrated species or hydroxides, and the free carboxylates that act as ligands.

We attempted to synthesize a series of PVM/Na-MA:Fe^{3+}-based hydrogels starting from a PVM/Na-MA solution at pH of 5.5. The PVM/Na-MA-to-Fe^{3+} ratio was in range of 10:1.25 to 10:5. At this starting pH, no hydrogel formed and only partial gels in the pH range of 2 to 4 were obtained instead. In the literature, Fe^{3+} hydrogels have been reported to form stable gels only at pH between 5.6 and 8.[1-3] A starting higher pH is required to deprotonate the carboxylate ligand.[3] Furthermore, Fe^{3+} ions are known to form mono-, bis- and tris- complexes with carboxylates depending on the pH of the solution.[1,4] The pH of the starting PVM/Na-MA solution was thus increased by opening the polymer anhydride with 2M NaOH. Table S1 presents the conditions of the PVM/Na-MA:Fe^{3+} synthesis starting from a PVM/Na-MA solution with pH between 7 and 7.5. Hydrogel formation was observed only when the ratios were 10:2 and 10:2.5 with pH of 6 and 5.5, respectively (Fig. S3). This is consistent with the lack of crosslinking between Fe^{3+} and carboxylates and the formation of only Fe^{3+} bis-complexes with the carboxylate at higher pH. When the pH of the starting PVM/Na-MA solution was increased to 10, most of the samples remained as solutions This is likely because of the formation of $Fe(OH)_3$ precipitate when starting from the PVM/Na-MA solution of pH 10 according to the probaix diagram of Fe in water.

Similarly, we tried to synthesize PVM/Na-MA:Al^{3+} hydrogels starting from PVM/Na-MA solution at the initial pH of 5.5 (1.5 M of NaOH) and 10 (3 M of NaOH). At pH of 5.5, no clear hydrogel formation was observed with a PVM/Na-MA:Al^{3+} molar ratio between 10:0.5 and 10:2. Instead, inhomogeneous gels were obtained that contained white precipitate. We attributed this white precipitate to the formation of aluminum oxide $Al_2O_3.H_2O$, which is dominant at this pH.[5] However, when a starting PVM/Na-MA solution at pH of 10 was used with $Al(NO_3)_3$, clear hydrogels were obtained for ratios of 10:3 and 10:4 (Fig. S4). Table S2 summarizes the synthesis conditions for aluminum hydrogels starting from a polymer stock solution at pH of 10. A similar pH effect was reported earlier for the formation of aluminum-based hydrogels with a starting pH of greater than 8.2.[1,6]

We also attempted to synthesize PVM/Na-MA:Ni^{2+}, PVM/Na-MA:Zn^{2+}, and PVM/Na-MA:Co^{2+} hydrogels. The molar ratio range was between 10:0.5 and 10:10 with all metal ions. The pH of the PVM/Na-MA solution was between 5.5 and 10. Only partial gelation was observed in nickel samples starting from pH of 7 to 7.5. No gel formation was observed with the PVM/Na-MA:Zn^{2+} and PVM/Na-MA:Co^{2+} samples at different pH

The inability to form hydrogels stems from the metal-to-carboxylate bond strength. The trend of the bond strength for carboxylates with divalent metals has been found to be Co(II)>Ni(II)>Zn(II)>Cu(II).[6] Hence the interaction of Co(II), Ni(II), and Zn(II) with PVM-Na/MA is weaker than with Cu(II), which may explain the absence of gelation with PVM-Na/MA. On the other hand, trivalent ions such as Fe^{3+} and Al^{3+} were capable of forming hydrogels in the suitable pH range, which was previously observed because trivalent ions have a stronger affinity for carboxylate groups.[6]

Rheological properties of Rheological properties of iron- and aluminum- based hydrogels

We also studied the rheological properties of PVM/Na-MA:Fe^{3+} hydrogels. The variations in the storage modulus (G') and loss modulus (G") as a function of frequency during frequency sweep measurements (Fig. S7) were compared for PVM/Na-MA:Fe^{3+} hydrogels with ratios of 10:2.5 and 10:2. We found that both hydrogels exhibited elastic behaviour as indicated by G' being

greater than G". The elastic modulus was found to be independent of frequency over the frequency range tested although G" decreased as the frequency increased. G' and G" of the sample with the 10:2.5 molar ratio were higher than G' and G" of the 10:2 sample. This is consistent with the formation of bis-complexation between Fe^{3+} and carboxylates.[1] The rheological properties of PVM/Na-MA:Fe^{3+} hydrogels were compared to those of PVM/Na-MA:Cu^{2+} with an optimal ratio 10:2.5 at the same starting pH. The iron-based hydrogel exhibited lower G' and G" than the Cu-based hydrogel exhibited. This confirms that the iron-based hydrogels were less rigid and less elastic in comparison with the copper-based hydrogels.

We also tested the rheological properties of PVM/Na-MA:Al^{3+} hydrogels. Both PVM/Na-MA:Al^{3+} hydrogels with ratios 10:3 and 10:4 exhibited constant G' during the frequency sweep measurements (Fig. S8). The G' of the sample with a molar ratio of 10:4 had higher G' than that of the 10:3 sample. However, in comparison with PVM/Na-MA:Cu^{2+} with an optimal ratio of 10:2.5, the aluminium samples were less elastic.

List of Figures and Tables

Table S1: Investigation of the synthesis conditions of PVM/Na-MA:$Fe(NO_3)_3$ with different ratios

Amount of Polymer (0.3 M [RU]) in mL	Amount of $Fe(NO_3)_3$ 0.75 M solution (mL)	Molar ratio (maleate within PVM/Na-MA:$Fe(NO_3)_3$)	Nature	pH
10	0. 5	10:1.5	Partial Gel	6
10	0.75	10:2	Gel	6
10	1	10:2.5	Gel	5.5
10	1.25	10:3	Partial Gel	4.5
10	1.5	10:4	Partial Gel	3
10	1.75	10:4.5	Partial Gel	2

Table S2: Investigation of the synthesis conditions of PVM/Na-MA:$Al(NO_3)_3$ with different ratios

Amount of Polymer (0.3 M [RU]) in mL (3 M NaOH)	Amount of $Al(NO_3)_3$ 0.75 M solution (mL)	Molar ratio (maleate within PVM/Na-MA: $Al(NO_3)_3$)	Nature	pH
10	0.75	10:2	Partial Gel	6.5
10	1.0	10:2.5	Partial Gel	6.5
10	1.25	10:3	Gel	6
10	1.5	10:4	Gel	6
10	1.75	10:4.5	Partial Gel	6
10	2.0	10:5	Partial Gel	6

Table S3 Investigation of Cu^{2+}-induced hydrogel formation PVM/Na-MA with various ratio of Nitrilotriacetic acid trisodium salt (NTA) (1 ml, concentration of NTA (M) at constant polymer amount (10 ml, 0.25 M), and $Cu(NO_3)_2$ (1 ml, 0.0625 M).

Sample Name	Nitrilotriacetic acid trisodium salt (NTA)		Nature by inversion test
	1 mL (M)	Final Conc. (M)	
10:0.01:2.5	0.003	0.00025	Gel
10:0.3:2.5	0.09	0.0075	Gel
10:0.7:2.5	0.20	0.0175	Gel
10:1.0:2.5	0.30	0.0250	Gel
10:1.3:2.5	0.40	0.0325	Gel
10:1.6:2.5	0.50	0.0400	Partial Gel
10:2:2.5	0.60	0.0500	No Gel

Table S4 Investigation of Cu^{2+} induced hydrogel formation PVM/Na-MA with various ratio of trisodium citrate (1 ml, concentration of trisodium citrate (M)) at constant polymer amount (10 ml, 0.25 M), and $Cu(NO_3)_2$ (1 ml, 0.0625 M).

Sample Name	Trisodium citrate salt		Nature by inversion test
	1 mL (M)	Final Conc. (M)	
10:0.05:2.5	0.015	0.00125	Gel
10:0.1:2.5	0.03	0.0025	Gel
10:0.2:2.5	0.06	0.0050	Gel
10:0.3:2.5	0.09	0.0075	Gel
10:0.7:2.5	0.20	0.0175	Partial Gel
10:1:2.5	0.30	0.0250	No Gel

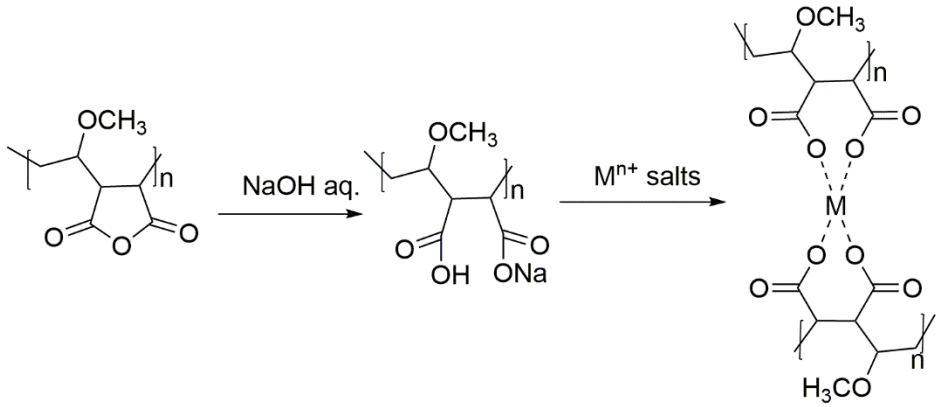

Fig. S1 The general scheme of the opening of the a Poly(methyl vinyl ether-alt-maleic anhydride) by NaOH aqueous solution and the addition of metal salts to form the polymeric metal carboxylates hydrogels.

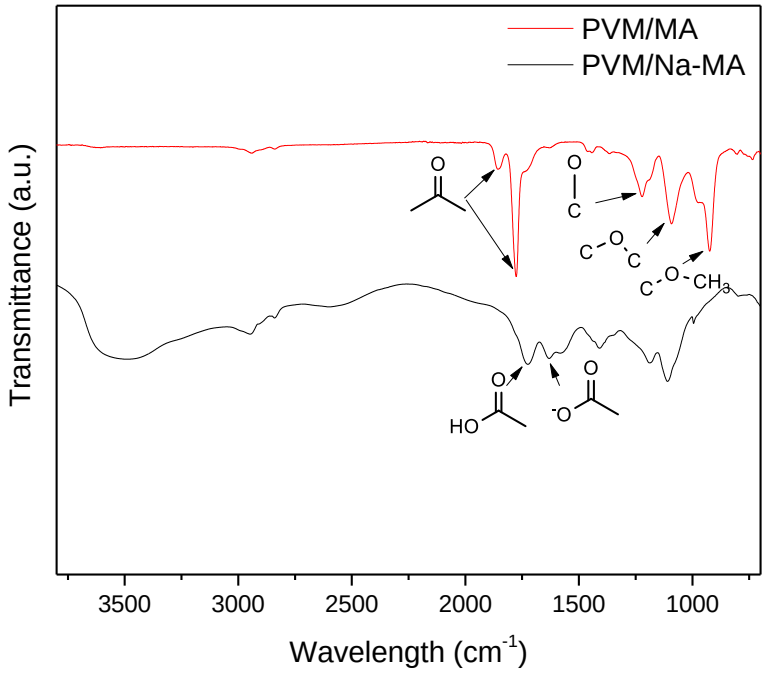

Fig. S2 FT-IR spectrum of PVM/MA (up) and PVM/Na-MA (down)

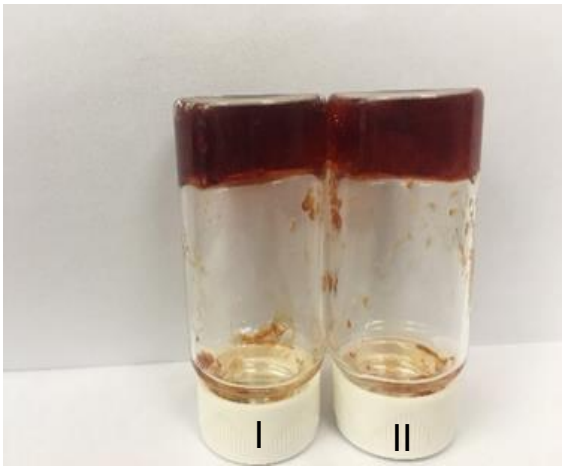

Fig. S3 An image of the PVM/Na-MA:$Fe(NO_3)_3$ hydrogels with ratios 10:2 (I) and 10:2.5 (II)

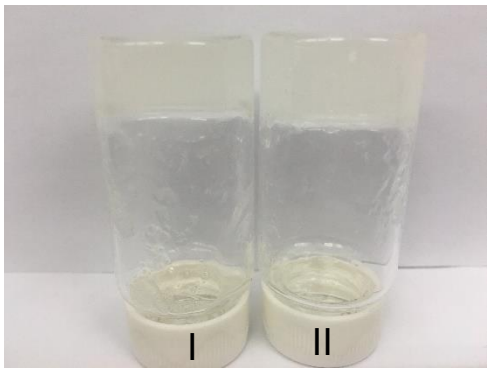

Fig. S4 An Image for PVM/Na-MA:$Al(NO_3)_3$ hydrogels prepared at ratios of 10:3 (I) and 10:4 (II).

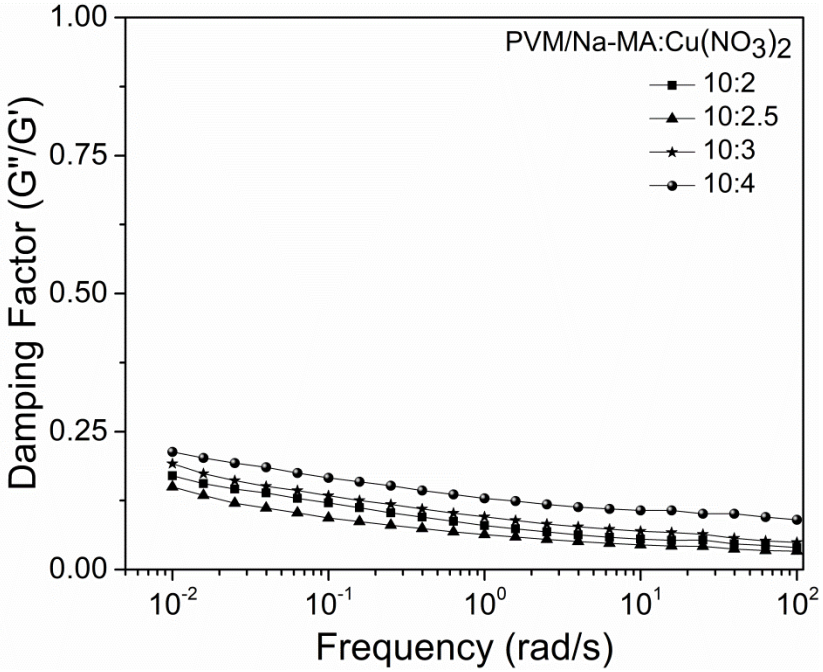

Fig. S5 Damping factor of hydrogels, as a function of frequency (frequency sweep) of PVM/Na-MA:$Cu(NO_3)_2$ with ratios 10:2,10:2.5, 10:3 and 10:4.

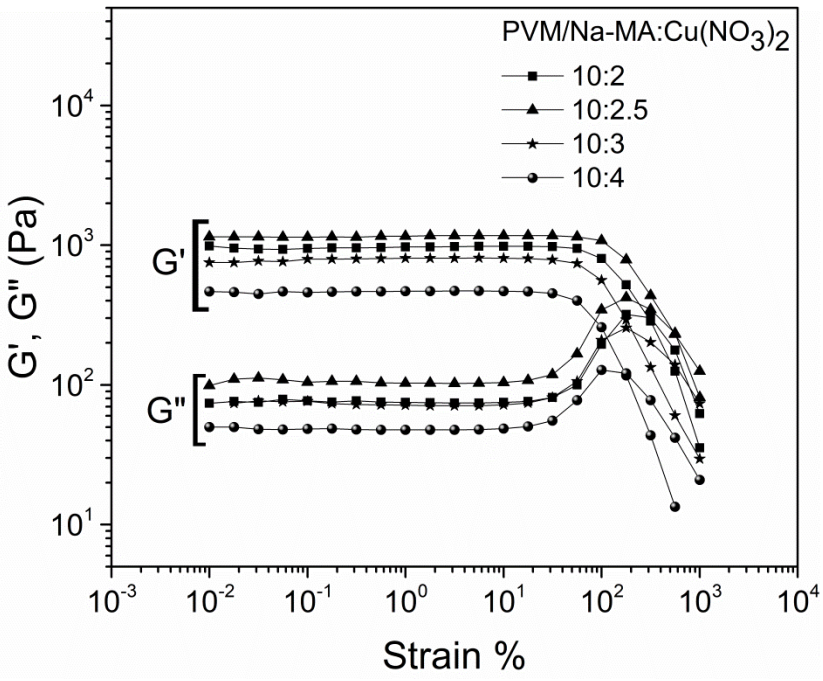

Fig. S6 storage modulus (G') loss modulus (G") as a function of strain obtained from amplitude sweep rheology of PVM/Na-MA:$Cu(NO_3)_2$ with ratios 10:2,10:2.5, 10:3 and 10:4.

Table S5: Investigation of hydrogel formation and rheological properties of "PVM/Na-MA stock solution" with various ratio $Cu(NO_3)_2$ aq. solution.

Sample. No	Amount of Polymer (0.3 M [RU]) in mL	Amount of $Cu(NO_3)_2$ 0.75 M solution (mL)	Molar ratio (maleate within PVM/Na-MA: PVM/Na-MA:$Cu(NO_3)_2$)	Nature	G'-G" (Pa)	Yield Stress (σ_y) (Pa)	Critical Strain (γ_c)	Critical Storage Modulus G'_c (Pa)	Cohesion Energy (E_c) (MJ/cm^3)
1	10	0.25	16:1	Solution	-	-	-	-	-
2	10	0.5	8:1	Partial Gel	-	-		-	-
3	10	0.75	5.3:1	Gel	352.4	437	306	303	14.18
4	10	1.0	4:1	Gel	557.2	487	550	370	55.96
5	10	1.25	3.2:1	Gel	245.0	353	226	237	6.05
6	10	1.5	2.6:1	Gel	171.8	230	175	122	1.86
7	10	1.75	2.3:1	Partial Gel	-	-	-	-	-
8	10	2.0	2:1	Precipitate	-	-	-	-	-

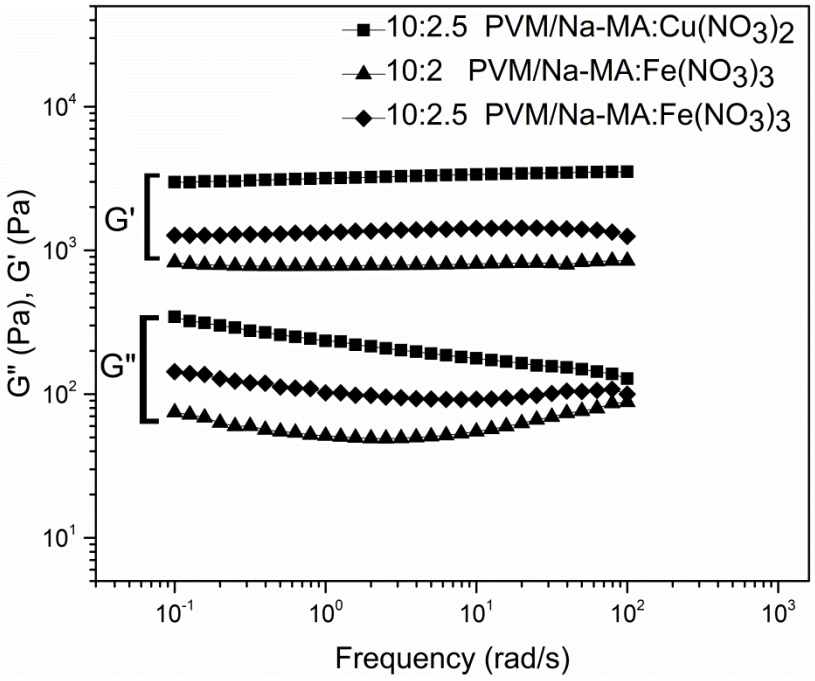

Fig. S7 Variation of (a) storage modulus (G') loss modulus (G") of PVM/Na-MA:$Fe(NO_3)_3$ with ratios 10:2 ,10:2.5 and PVM/Na-MA:$Cu(NO_3)_2$ with ratio of 10:2.5.

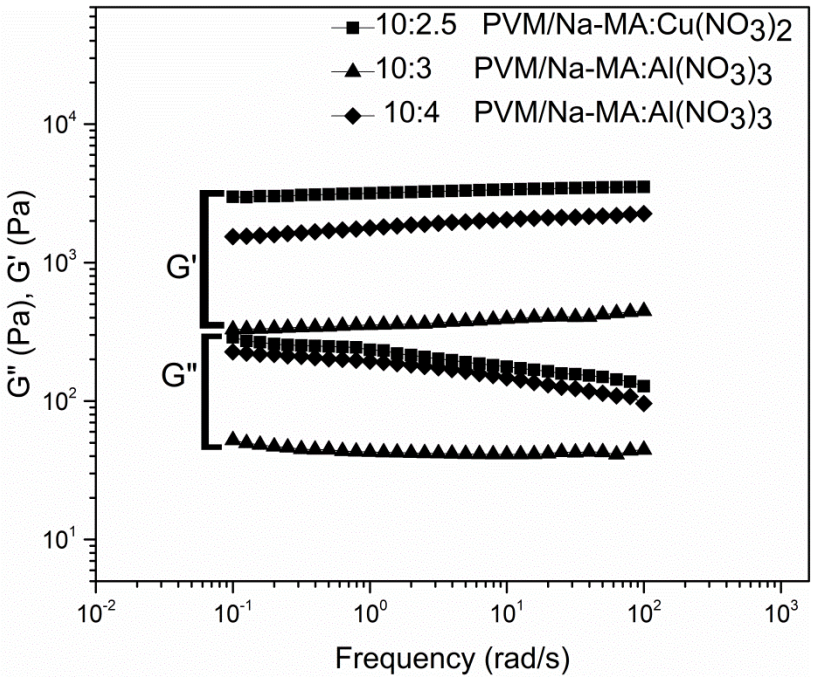

Fig. S8 Variation of storage modulus (G') loss modulus (G") of PVM/Na-MA:$Al(NO_3)_3$ with ratios 10:3 and 10:4 and PVM/Na-MA:$Cu(NO_3)_2$ with ratio of 10:2.5.

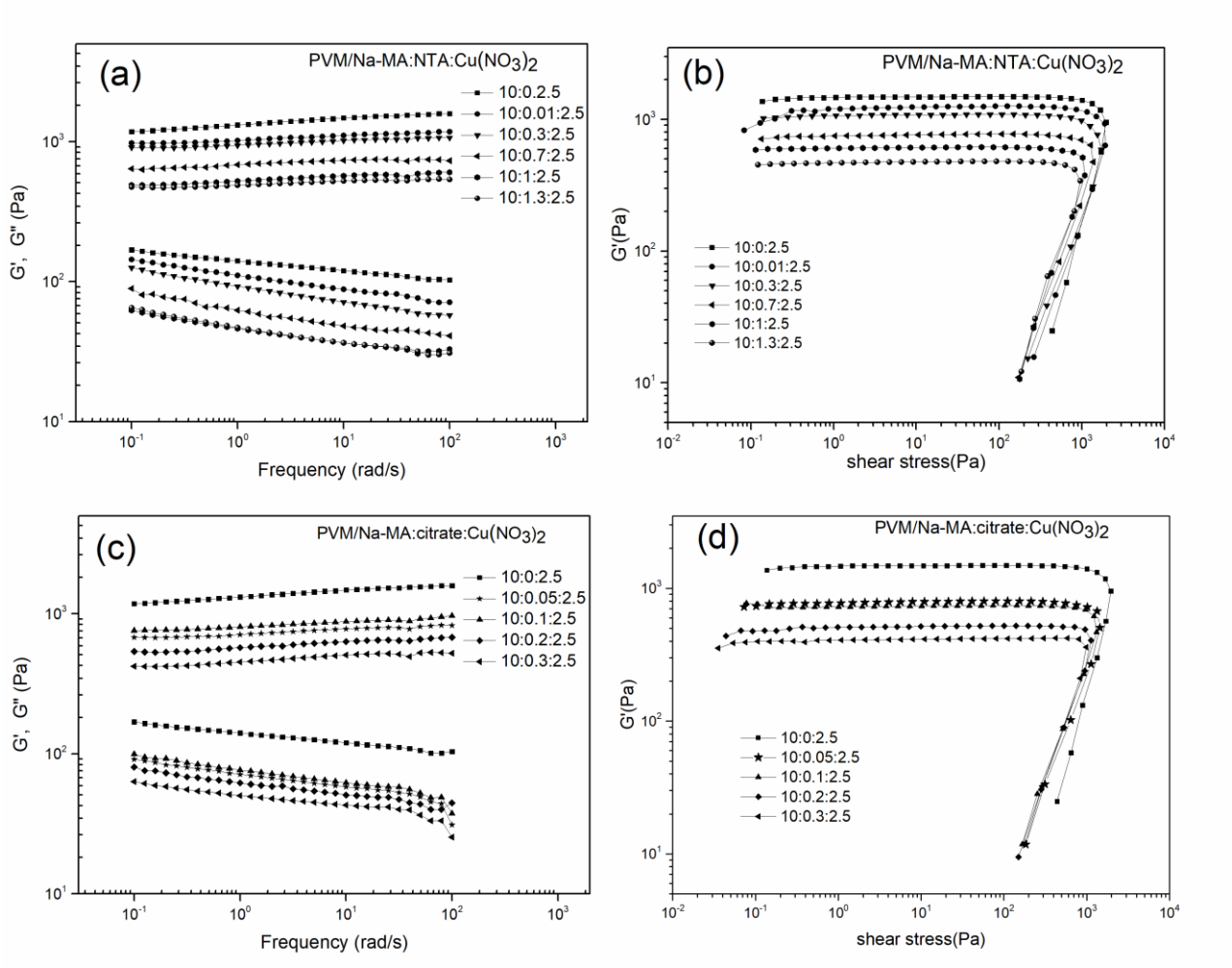

Fig. S9 (a, c) Variation of storage modulus (G') loss modulus (G") as a function of frequency (frequency sweep) (b,d) storage modulus (G') as a function of shear stress (amplitude sweep) for hydrogels with different ratios of NTA and citrate spacer ligands.

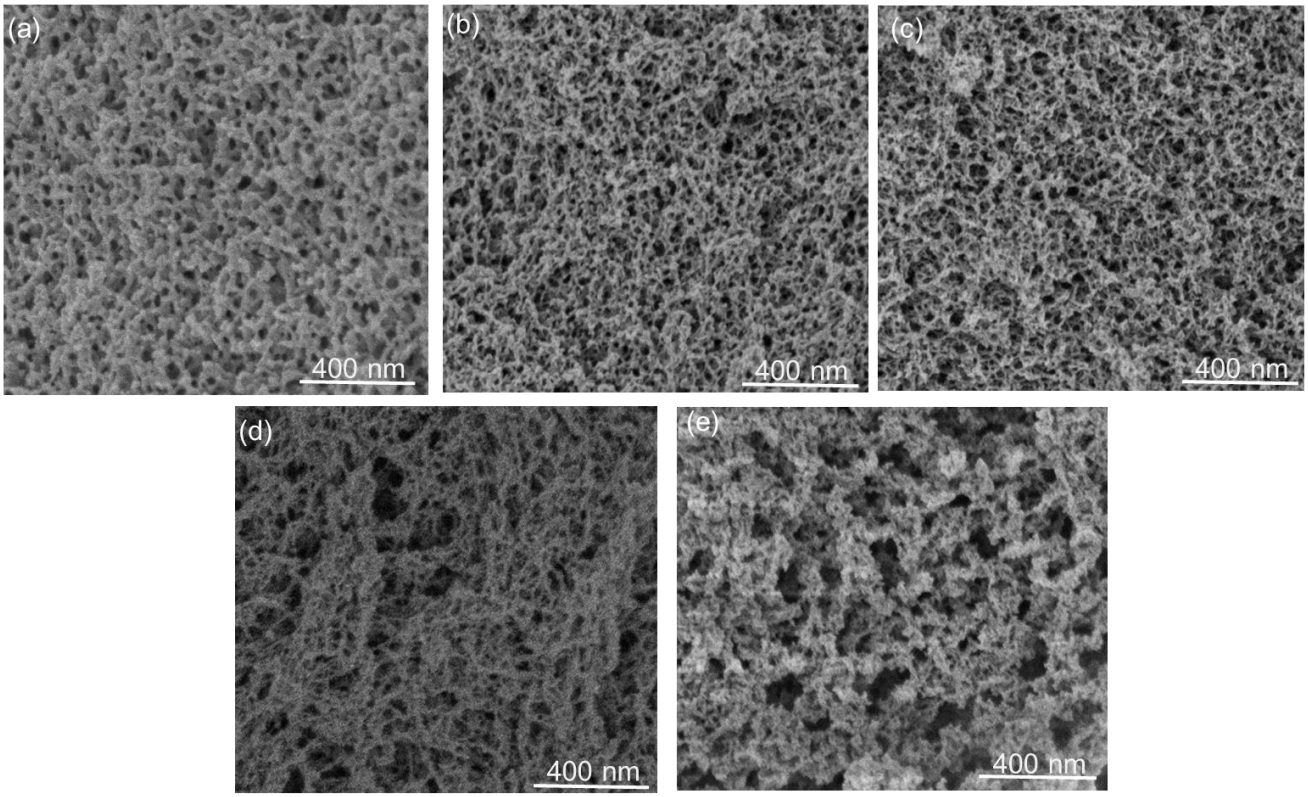

Fig. S10 SEM images of (a) 10:0:2.5, (b) 10:1:2.5, (c) 10:2:2.5, (d) 10:3:2.5, and (e) 10:4:2.5, PVM/Na-MA:adipate:$Cu(NO_3)_2$ hydrogels after critically point drying with CO_2.

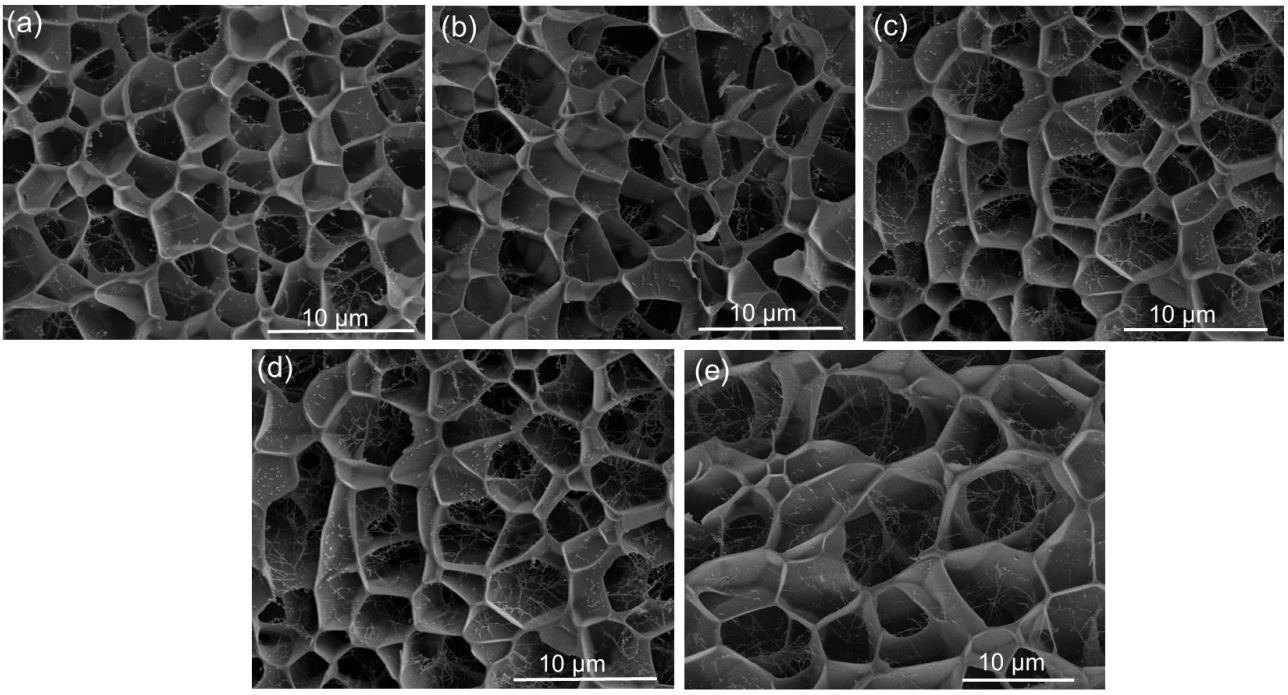

Fig. S11 Cryo-SEM images of (a) 10:0:2.5, (b) 10:1:2.5, (c) 10:2:2.5, (d) 10:3:2.5, and (e) 10:4:2.5, PVM/Na-MA:adipate:$Cu(NO_3)_2$ intact hydrogels.

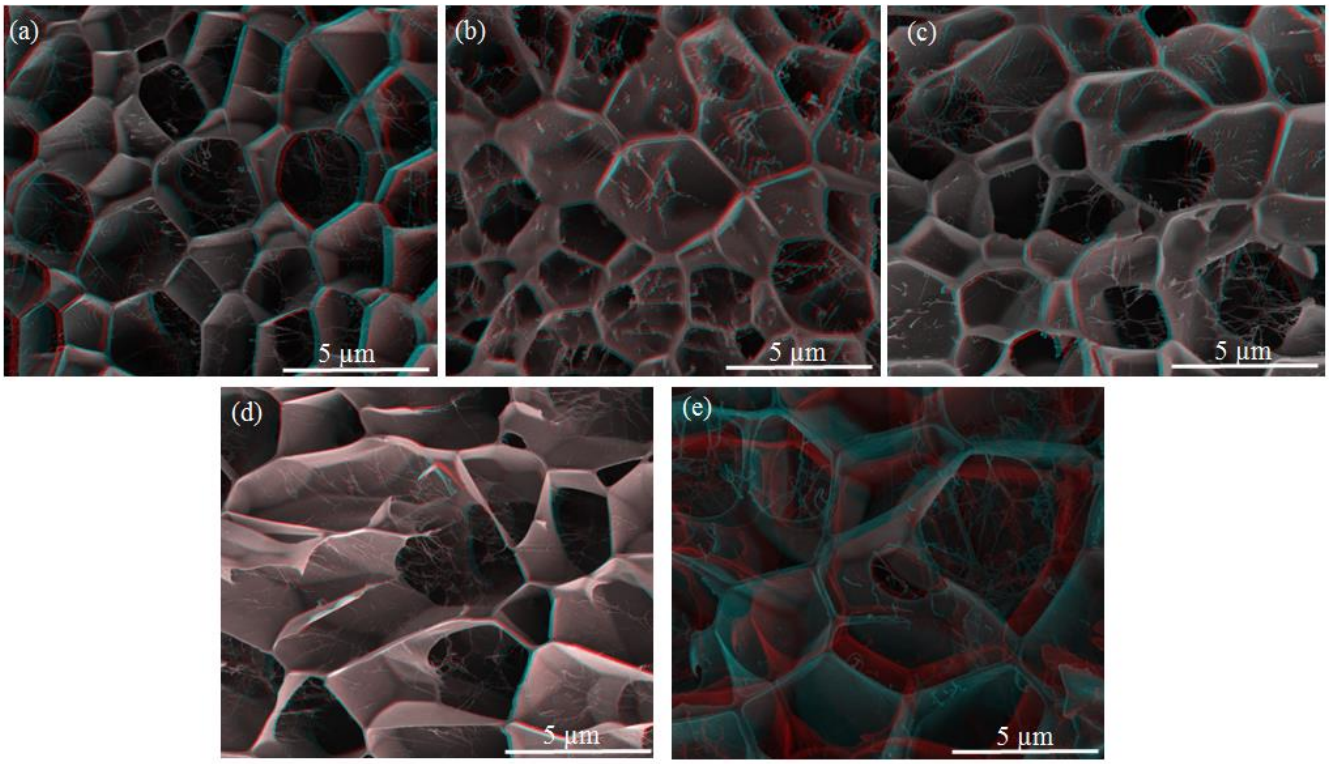

Fig. S12 3D Cryo-SEM images of (a) 10:0:2.5, (b) 10:1:2.5, (c) 10:2:2.5, (d) 10:3:2.5, and (e) 10:4:2.5, PVM/Na-MA:adipate:$Cu(NO_3)_2$ intact hydrogels.

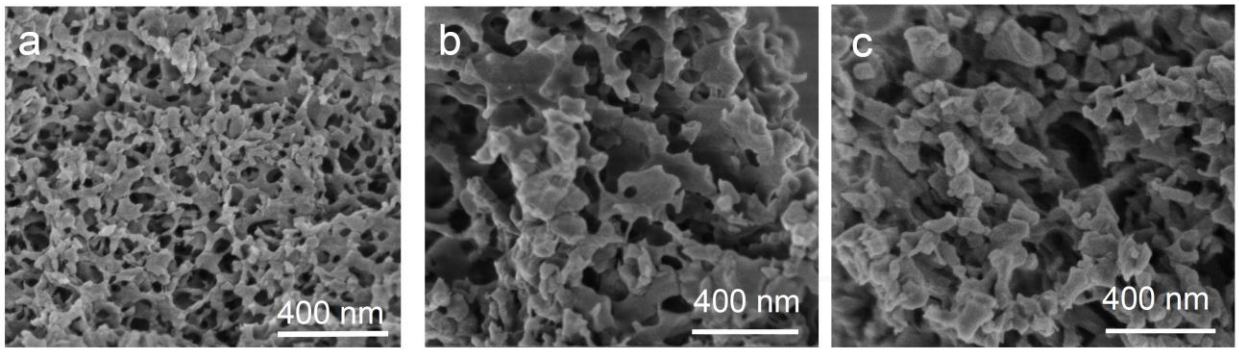

Fig. S13 SEM images of a) 10:0.01:2.5, b) 10:1:2.5 and c) 10:1.3:2.5 PVM/Na-MA:NTA:$Cu(NO_3)_2$ hydrogels after critically point drying with CO_2.

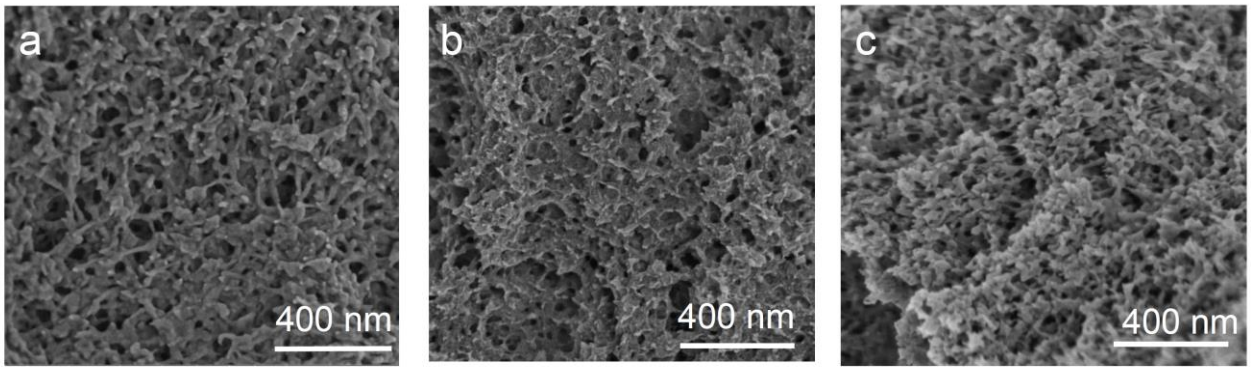

Fig. S14 SEM images a) 10:0.05:2.5, b) 10:0.2:2.5 and c) 10:0.3:2.5 PVM/Na-MA:citrate:$Cu(NO_3)_2$ hydrogels after critically point drying with CO_2.

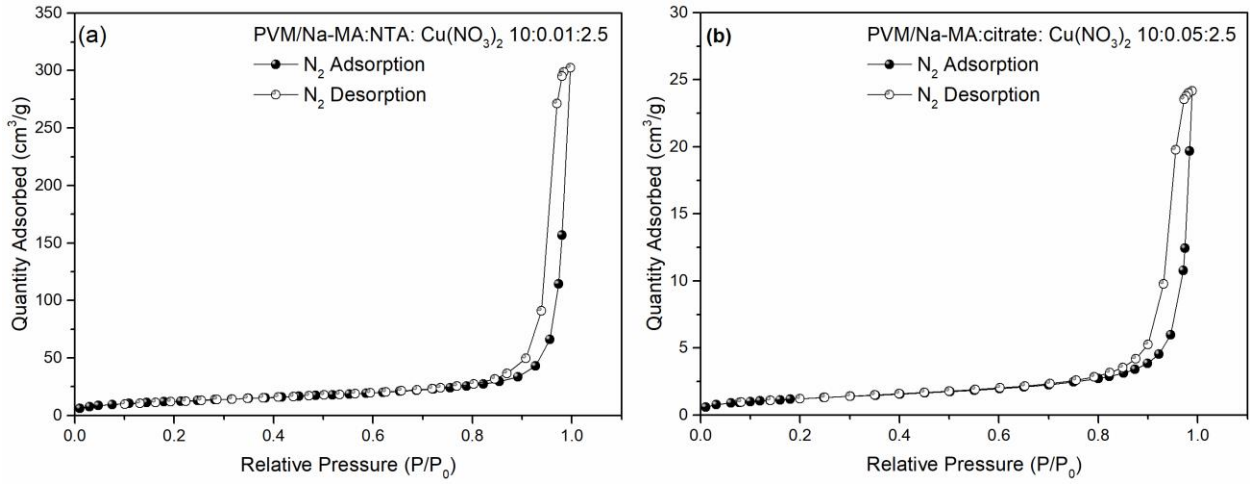

Fig. S15 Nitrogen adsorption-desorption isotherm of a) PVM/Na-MA:NTA:$Cu(NO_3)_2$ with ratio 10:0.01:2.5, (b) PVM/Na-MA: citrate: $Cu(NO_3)_2$ with ratio 10:0.05:2.5 hydrogels.

Table S6 Summary of Surface area, Pore volume, and N_2 uptake capacity of the hydrogels with NTA and citrate spacer ligands.

Sample	Surface Area ($m^2\ g^{-1}$)	Pore Volume ($cm^3\ g^{-1}$)	N_2 Uptake ($cm^3\ g^{-1}$)
10:0.01:2.5 (NTA)	44.46	0.46	303
10:0.05:2.5(citrate)	116.94	0.47	24.17

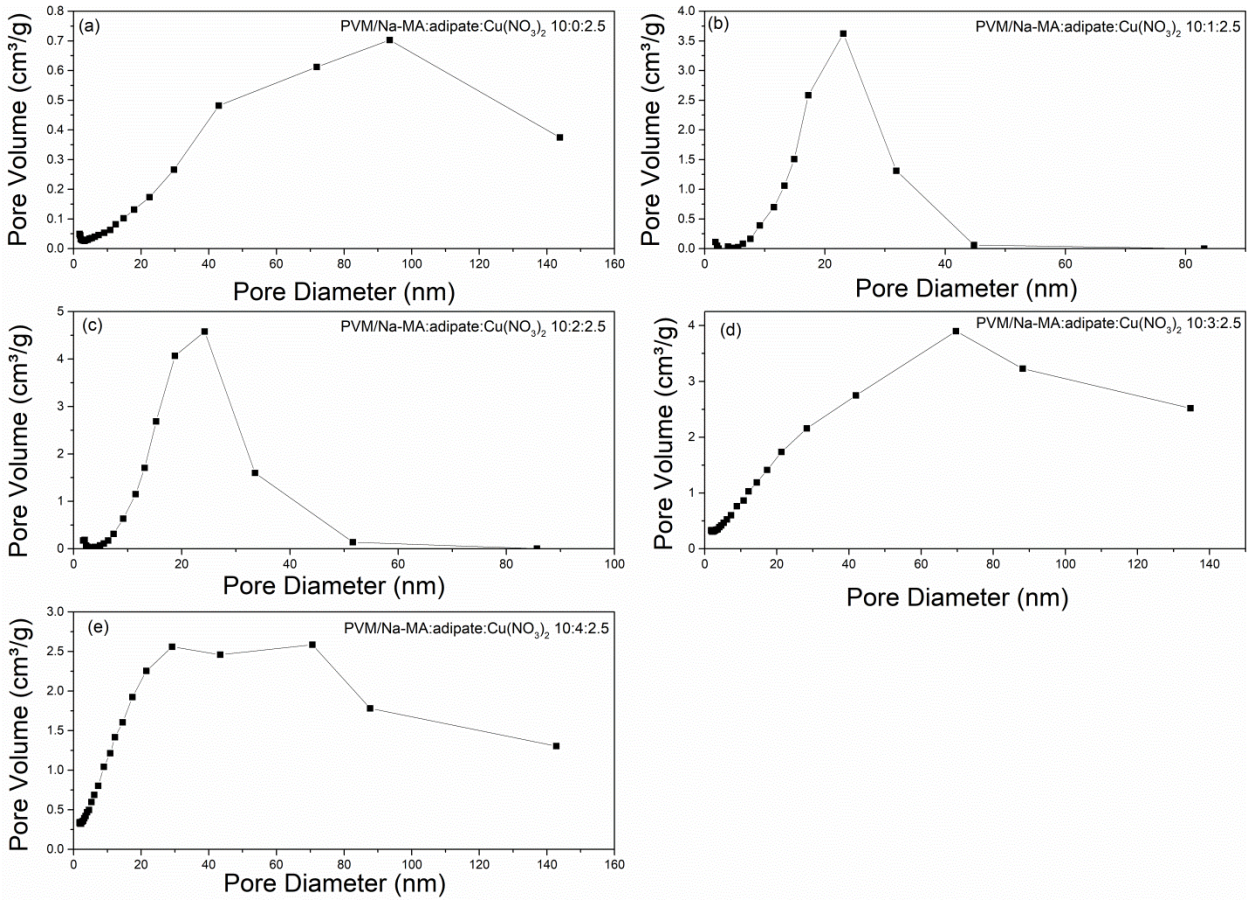

Fig. S16 Pore-size (V-D) distribution plot calculated from the adsorption isotherm by the BJH method for PVM/Na-MA:adipate:$Cu(NO_3)_2$ (a) 10:0:2.5, (b) 10:1:2.5, (c) 10:2:2.5, (d) 10:3:2.5, and (e) 10:4:2.5 hydrogels.

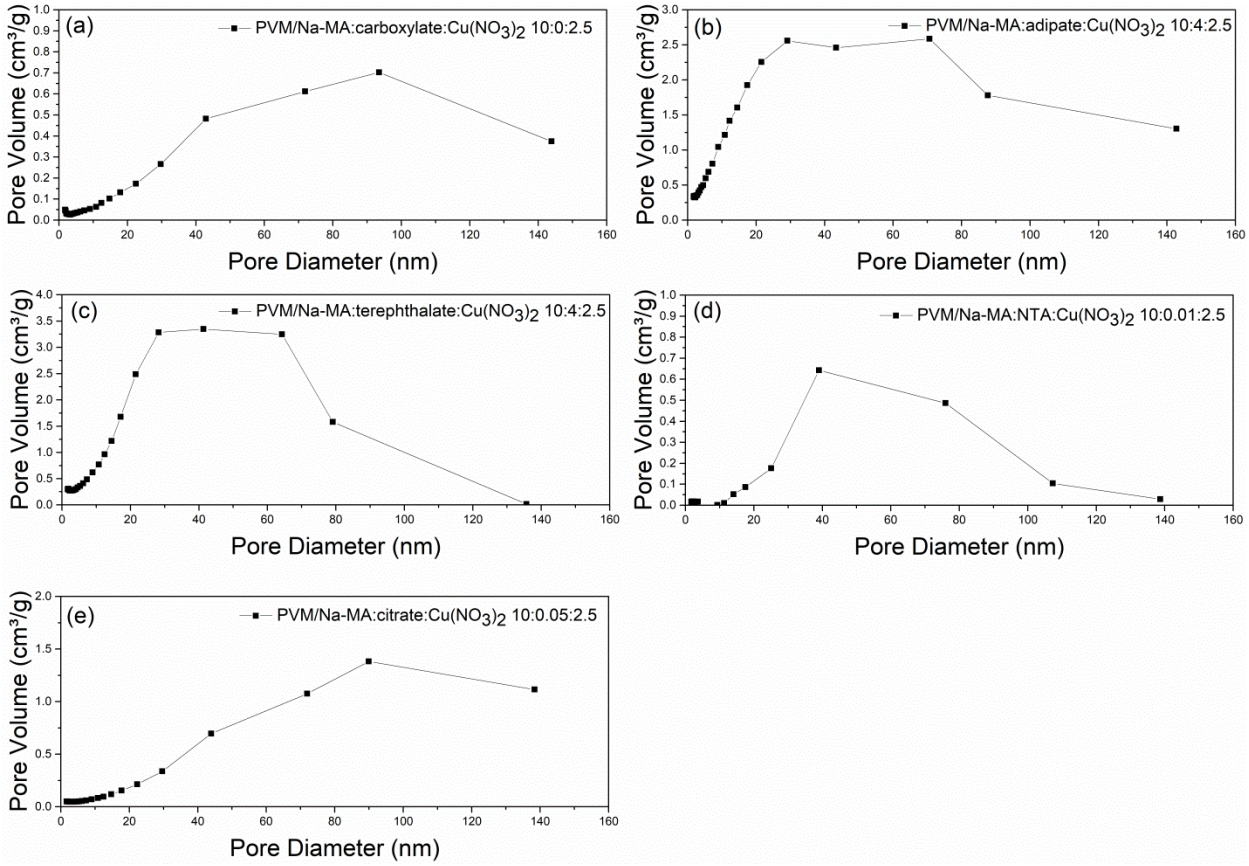

Fig. S17 Pore-size (V-D) distribution plot calculated from the adsorption isotherm by the BJH method for (a) PVM/Na-MA:carboxylate:$Cu(NO_3)_2$ 10:0:2.5, (b) PVM/Na-MA:adipate:$Cu(NO_3)_2$ 10:4:2.5, (c) PVM/Na-MA:terephthalate:$Cu(NO_3)_2$ 10:4:2.5, (d) PVM/Na-MA:NTA:$Cu(NO_3)_2$ 10:0.01:2.5 and (e) PVM/Na-MA:citrate:$Cu(NO_3)_2$ 10:0.05:2.5 hydrogels.

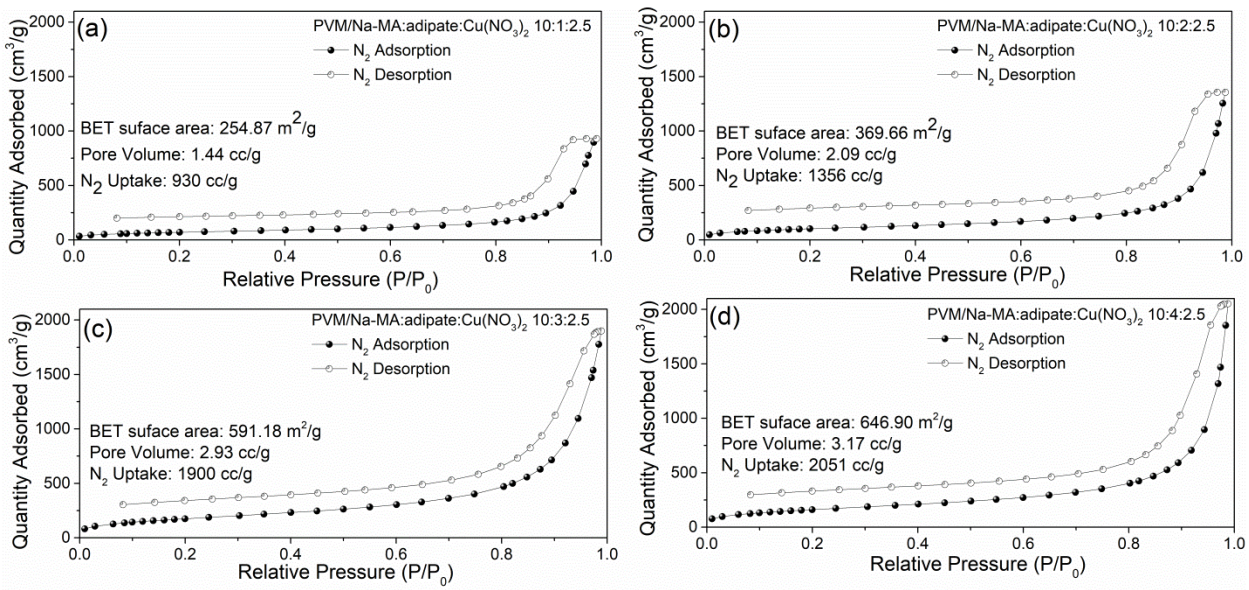

Fig. S18 Nitrogen adsorption-desorption isotherm of PVM/Na-MA:adipate:$Cu(NO_3)_2$ (a) 10:1:2.5, (b) 10:2:2.5, (c) 10:3:2.5, and (d) 10:4:2.5 hydrogels.

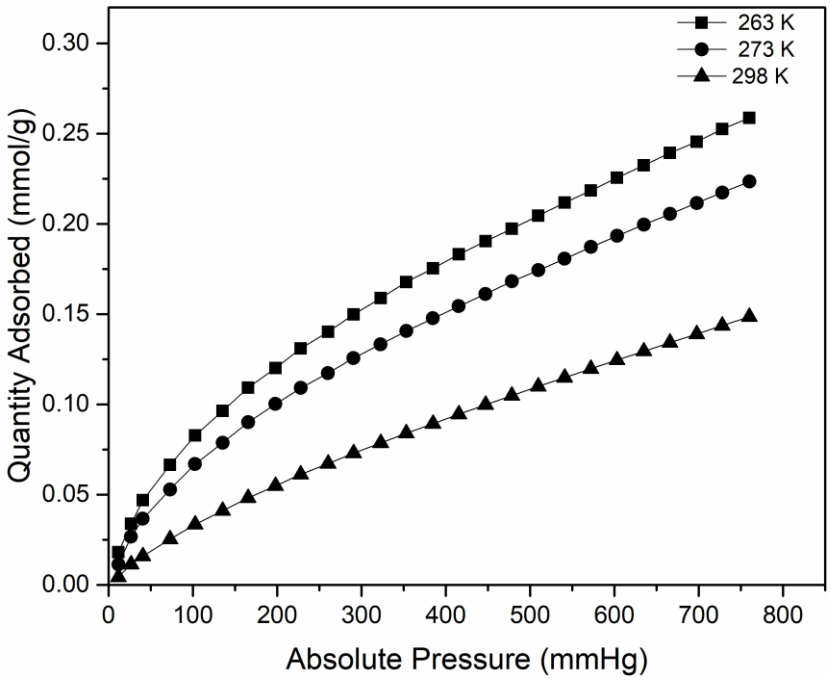

Fig. S19 CO_2 Gas adsorption isotherms for PVM/Na-MA:adipate:$Cu(NO_3)_2$ of 10:4:2.5 ratio at different temperatures of 263, 273 and 298 K in a pressure range between 0 and 760 mmHg.

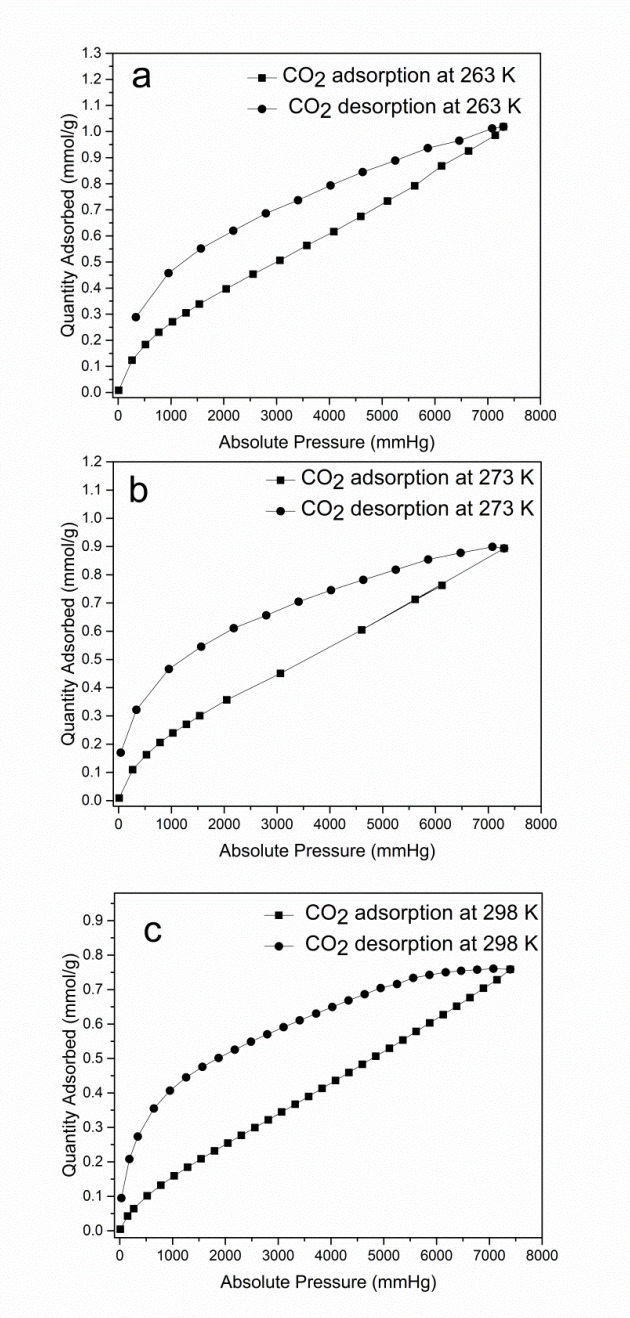

Fig. S20 CO_2 Gas adsorption-desorption isotherms of PVM/Na-MA:adipate: $Cu(NO_3)_2$ of 10:4:2.5 ratio at different temperatures of 263, 273 and 298 K in a pressure range between 0 and 7600 mmHg.

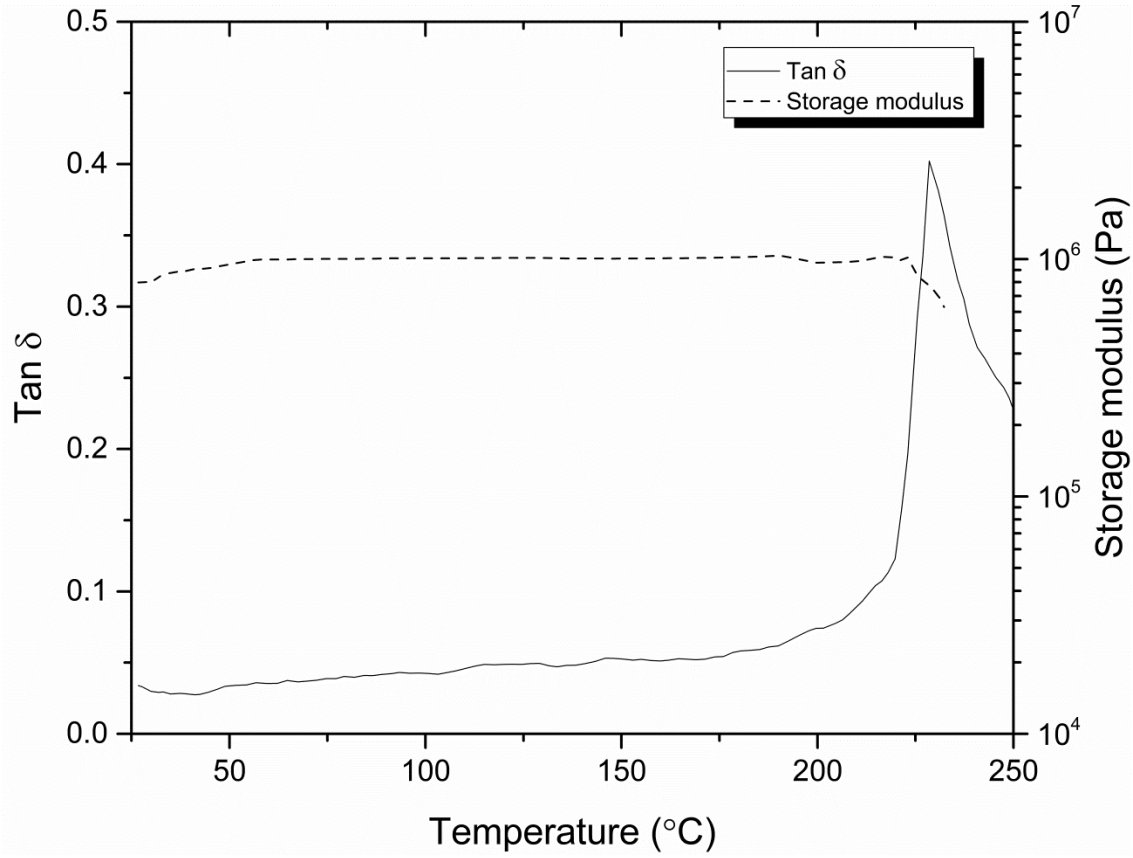

Fig. S21 Typical DMA response showing storage modulus and tan δ as a function of temperature for critically dried powders of PVM/Na-MA:adipate:$Cu(NO_3)_2$ 10:4:2.5. .

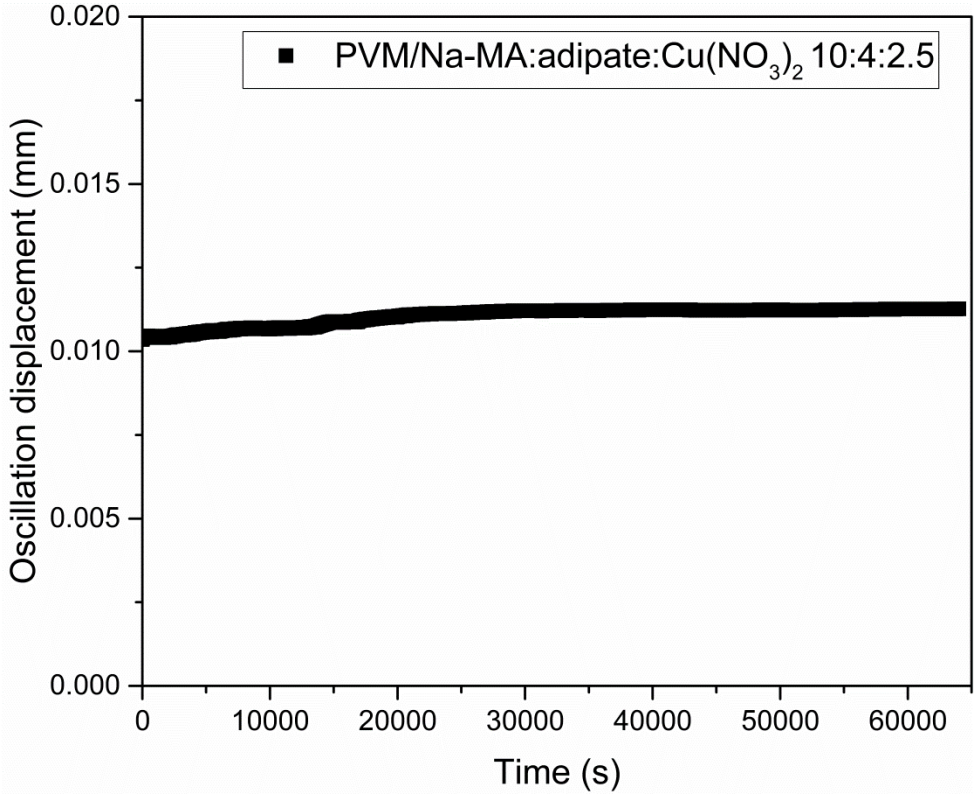

Fig. S22 Variation of oscillation displacement as a function of time for PVM/Na-MA:adipate: $Cu(NO_3)_2$ with 10:4:2.5 ratio.

References

1 N. Holten-Andersen, M. J. Harrington, H. Birkedal, B. P. Lee, P. B.Messersmith, K. Y. C. Lee and J. H. Waite, *Proc. Natl. Acad. Sci.,* 2011, **108,** 2651-2655.
2 M. S. Menyo, C. J. Hawker and J. H.Waite, *ACS Macro Lett.,* 2015, **4,** 1200-1204.
3 Z. Wei, J. He, T. Liang, H. Oh, J. Athas, Z. Tong, C. Wang and Z. Nie, *Polym. Chem.,* 2013, **4,** 4601-4605.
4. N. Holten-Andersen, A. Jaishankar, M. J. Harrington, D. E. Fullenkamp, G. DiMarco, L. He, G. H. McKinley, P. B. Messersmith and K. Y. C. Lee, *J. Mater.Chwm.,* 2014, **2,** 2467-2472.
5. M. Pourbaix, A*tlas of electrochemical equilibria in aqueous solutions*, Pergamon, New York, 1966.
6. K. J. Henderson, T. C. Zhou, K. J. Otim and K. R. Shull, *Macromolecules,* 2010, **43,** 6193-6201.